

1 Elucidating Adsorptive Fractions of Natural Organic Matter on 2 Carbon Nanotubes

3 Mohamed Ateia,^{*,†,‡} Onur G. Apul,^{‡,§} Yuta Shimizu,[†] Astri Muflihah,[†] Chihiro Yoshimura,[†]
4 and Tanju Karanfil^{||}

5 [†]Department of Civil and Environmental Engineering, Tokyo Institute of Technology, 2-12-1-M1-4 Ookayama, Tokyo 152-8552,
6 Japan

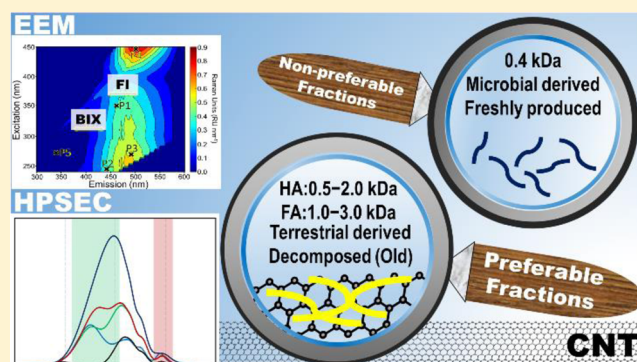
7 [‡]Department of Civil and Environmental Engineering, University of Massachusetts Lowell, Lowell, Massachusetts 01854, United
8 States

9 [§]School of Sustainable Engineering and the Built Environment, Arizona State University, Tempe, Arizona 85259, United States

10 ^{||}Department of Environmental Engineering and Earth Sciences, Clemson University, Anderson, South Carolina 29625, United States

11 **S** Supporting Information

12 **ABSTRACT:** Natural organic matter (NOM) is a heteroge-
13 neous mixture of organic compounds that is omnipresent in
14 natural waters. To date, the understanding of the adsorption of
15 NOM components by carbon nanotubes (CNTs) is limited
16 because of the limited number of comprehensive studies in the
17 literature examining the adsorption of NOM by CNTs. In this
18 study, 11 standard NOM samples from various sources were
19 characterized, and their adsorption behaviors on four different
20 CNTs were examined side-by-side using total organic carbon,
21 fluorescence, UV–visible spectroscopy, and high-performance
22 size-exclusion chromatography (HPSEC) analysis. Adsorption
23 was influenced by the chemical properties of the NOM,
24 including aromaticity, degree of oxidation, and carboxylic
25 acidity. Fluorescence excitation–emission matrix (EEM) analysis showed preferential adsorption of decomposed and terrestrial-
26 derived NOM compared to freshly produced and microbial-derived NOM. HPSEC analysis revealed preferential adsorption of
27 fractions in the molecular weight range of 0.5–2 kDa for humic acids but in the molecular weight range of 1–3 kDa for all fulvic
28 acids and reverse-osmosis isolates. However, the smallest characterized fraction (MW < 0.4 kDa) in all samples did not adsorb on
29 the CNTs.



1. INTRODUCTION

30 Natural organic matter (NOM) is ubiquitous in fresh waters
31 and is found in concentrations that range from 1–2 (mg of C)/
32 L to 40 (mg of C)/L depending on the source and climate.^{1,2}
33 The presence of NOM, which is a mixture of complex
34 polyelectrolytes, during water treatment processes presents a
35 broad range of problems, such as an increase in chemical
36 demands, the formation of disinfection byproducts, the
37 occurrence of taste and odor problems, and the fouling of
38 activated carbons and membranes.^{3,4} Therefore, several
39 processes have been employed to remove NOM from water,
40 including coagulation, membrane filtration, ion exchange,
41 advanced oxidation processes, and adsorption.⁵
42 Carbon nanotubes (CNTs), with their high surface areas,
43 hydrophobicity, porosity, and rapid sorption kinetics, have been
44 explored as one of the next-generation adsorbents.^{6,7} Over the
45 past decade, extensive studies have investigated applications of
46 CNTs in the adsorption of several organic and inorganic water
47 contaminants.^{8,9} Furthermore, the interactions between CNTs
48 and NOM have been examined in some studies.^{1,10–17}

49 Mechanisms for the adsorption of NOM components by
50 CNTs include hydrophobic interactions, π – π interactions, 50
51 hydrogen-bonding interactions, and electrostatic interac-
52 tions.^{10,18} These interactions are influenced by (1) the
53 characteristics of the CNTs (e.g., surface area, pore volume,
54 and surface functionalities),^{10,14,19} (2) the NOM molecular
55 structure and composition (e.g., molecular weight and
56 size),^{13,19} and (3) the solution chemistry (e.g., pH, water
57 temperature, and ionic strength).^{1,10}

58 It was also reported that the conformation and composition
59 of the NOM remaining in water will change as a result of
60 adsorption processes due to NOM fractionation.^{15,20} However,
61 there are no comprehensive studies in the literature examining
62 the adsorption of NOM by CNTs. The limited observations in
63 previous studies are due to a number of factors: (1) different

Received: March 9, 2017

Revised: May 21, 2017

Accepted: May 24, 2017

Published: May 24, 2017

Table 1. Types, Codes, and Selected Physicochemical and Fluorescence Properties of Natural Organic Matter Samples Used in This Study

code	catalog no.	SUVA ₂₅₄ ^b [L/(mg m)]	M _w ^c (kDa)	M _n ^c (kDa)	ρ ^d	EEM ^a indexes		
						FI ^e	BIX ^f	
Humic Acids								
ESHA	4S102H	6.2	5.8	1.0	5.8	0.84	0.25	
PPHA	1S103H	6.9	6.2	1.5	4.2	0.86	0.24	
LHA	1S104H	7.0	4.8	1.0	4.8	0.94	0.28	
SRHA	2S101H	4.9	3.9	1.4	2.7	1.00	0.25	
Fulvic Acids								
SRFA1	2S101F	3.5	1.8	1.0	1.8	1.19	0.27	
SRFA2	1S101F	4.0	1.8	1.2	1.5	1.16	0.24	
PPFA	2S103F	3.9	1.4	0.9	1.7	1.29	0.30	
NLFA	1R105F	4.6	1.8	1.0	1.8	1.20	0.28	
RO Isolates								
NNOM	1R108N	3.6	1.3	0.6	1.9	1.33	0.31	
MNOM	1S110N	2.6	1.3	0.7	1.7	1.49	0.39	
SNOM	1R101N	3.3	1.5	0.8	1.8	1.34	0.30	

^aExcitation–emission matrix. ^bSpecific UV absorption (SUVA) values were calculated by dividing the UV absorbance at 254 nm (m⁻¹) by the dissolved organic carbon (DOC) concentration (mg/L). ^cWeight-average molecular weight (M_w) and number-average molecular weight (M_n) measured using HPSEC. ^dPolydispersity (ρ) calculated as M_w/M_n. ^eFluorescence index (FI) calculated as the ratio of the emission intensity at Em 450 nm relative to that at Em 500 nm at Ex 370 nm. ^fFreshness index (BIX) calculated by taking the intensity ratio of Em 380 nm relative to Em 430 nm at Ex 310 nm.

Table 2. Characteristics of All Carbon Nanotubes Used in This Study

code	type	SA ^a (m ² /g)	PV _{total} ^a (cm ³ /g) [%]	PV _{micro} ^a (cm ³ /g) [%]	PV _{meso} ^a (cm ³ /g) [%]	PV _{macro} ^a (cm ³ /g) [%]	OD ^b (nm)	oxygen content ^c (wt %)	purity ^b (%)	supplier
C1	MWCNTs	136	0.45 [100]	0.02 [4]	0.34 [68]	0.14 [28]	3–20	0.30	>95	Wako Chemicals, Japan
C2	SWCNTs	380	0.9 [100]	0.05 [5]	0.81 [91]	0.04 [4]	1–2	1.32	>90	Alpha Nano, Chinese Academy of Science, China
C3	MWCNTs	114	0.47 [100]	0.02 [3]	0.36 [65]	0.18 [32]	5–10	0.21	>98	Alpha Nano, Chinese Academy of Science, China
C4	MWCNTs	96	0.4 [100]	0.01 [2]	0.34 [76]	0.10 [22]	10–20	0.25	>98	Alpha Nano, Chinese Academy of Science, China

^aBET surface areas, pore volumes and pore size distributions were measured from nitrogen physisorption data at 77 K obtained with ASAP 2020 analyzer (Micromeritics Instrument Corp., Norcross, GA). SA is surface area, PV_{total} is the total pore volume, PV_{micro} is the volume of micropores (i.e., PV < 2 nm), PV_{meso} is the volume of mesopores (i.e., 2 nm < PV < 50 nm), and PV_{macro} is the volume of macropores (i.e., PV > 50 nm). ^bInformation provided by the suppliers. ^cOxygen contents analyzed using a Flash Elemental Analyzer 1112 series (Thermo Electron Corporation).

64 types of NOM used in these studies (i.e., different chemical and
65 physical characteristics), (2) limitations in the number of NOM
66 samples tested under different experimental conditions, and (3)
67 limited and different techniques employed in NOM character-
68 ization [e.g., high-performance size-exclusion chromatography
69 analysis (HPSEC)]^{10,12} vs E2/E3 (UV absorbance at 250 nm/
70 365 nm) and E4/E6 (UV absorbance at 465 nm/665 nm)].^{11,15}

71 In this study, our objective was to systematically investigate
72 the adsorption behavior of 11 NOM samples from various
73 sources by performing isotherm and kinetic experiments and
74 using a suite of NOM characterization techniques (total organic
75 carbon, fluorescence, UV–vis spectroscopy, and HPSEC). The
76 results provide a more robust understanding of the adsorption
77 behavior of NOM samples on CNTs in natural waters and the
78 potential applications for water treatment.

2. MATERIALS AND METHODS

79 **2.1. Materials.** Four standard humic acids [Elliott Soil IV
80 (ESHA), Pahokee Peat (PPHA), Leonardite (LHA), and
81 Suwannee River II (SRHA)], four standard fulvic acids
82 [Suwannee River II (SRFA1), Suwannee River I (SRFA2),
83 Pahokee Peat II (PPFA), and Nordic Lake (NLFA)], and three
84 reverse-osmosis (RO) isolates [Nordic Reservoir (NNOM),

Upper Mississippi River (MNOM), and Suwannee River 85
(SNOM)] were purchased from the International Humic 86
Substances Society (IHSS). The chemical properties of the 87
NOM samples, including elemental composition/ratio, carbon 88
species, concentrations of acidic functional groups, fluorescence 89
indexes, and average molecular weights, are listed in Tables 1 90
and S1. 91

Three different types of multiwalled carbon nanotubes 92
(MWCNTs) and one type of single-walled carbon nanotubes 93
(SWCNTs) were purchased from Wako Pure Chemicals, 94
Osaka, Japan, and Alpha Nano Technology Co., Chinese 95
Academy of Science, Chengdu, China. The characteristics of all 96
carbon nanotubes used in this study are listed in Table 2. The 97
Brunauer–Emmett–Teller (BET) surface areas, pore volumes, 98
and pore size distributions were measured from nitrogen 99
physisorption data obtained at 77 K with an ASAP 2020 100
analyzer (Micromeritics Instrument Corp., Norcross, GA). The 101
oxygen contents of the adsorbents were analyzed using a Flash 102
Elemental Analyzer 1112 series (Thermo Electron Corpo- 103
ration). 104

2.2. Preparation of NOM Solutions. NOM samples (25– 105
50 mg) were dissolved in a 0.01 M NaOH solution to prepare a 106
stock solution of 10 g/L. The pH of each NOM solution was 107

adjusted to 7.0 ± 0.2 with 0.01 M HCl or 0.01 M NaOH. The volume of acid or alkali solution was recorded and was taken into account during the calculation of the final NOM concentration. All stock solutions were stored in the dark and refrigerated ($4\text{ }^{\circ}\text{C}$), when not in use.

2.3. Adsorption Isotherms. Batch reactors were used to perform adsorption experiments. Each NOM stock solution was diluted with 1 mM phosphate buffer solution and then adjusted to $\text{pH } 7.0 \pm 0.2$. Based on preliminary kinetic experiments, the equilibrium time was set at 24 h [section S1 in the Supporting Information (SI)]. Adsorption isotherm experiments were carried out under different conditions: (1) constant CNT dose and variable NOM concentration (2.5–60 mg/L) and (2) variable CNT dose [125–500 (mg of CNTs)/L] and constant NOM concentration. At the end of the equilibrium time, samples were collected, filtered [with a prewashed $0.45\text{-}\mu\text{m}$ polyethersulfone (PES) filter, Membrane Solutions, Tokyo, Japan], and kept refrigerated until further measurements. The adsorbed NOM amounts [measured as dissolved organic carbon (DOC)] were determined by subtracting the concentration of dissolved NOM remaining in the solution from the initial concentration. Each isotherm point was measured in triplicate, and variations are reported as standard errors. Blank experiments (with no adsorbents) were conducted in parallel, and the changes in NOM concentration in the blanks were found to be negligible.

2.4. Analysis. DOC concentrations were quantified using a total organic carbon (TOC) analyzer (Shimadzu V-series, TOC-CHP, Kyoto, Japan). The UV absorbance at 254 nm was obtained with a UV–visible spectrophotometer (Shimadzu UV-1800, Kyoto, Japan). The specific UV absorption (SUVA_{254}) values were calculated by dividing the UV absorbance at 254 nm (m^{-1}) by the DOC concentration (mg/L). The average molecular weights of all samples were determined using a high-performance size-exclusion chromatography (HPSEC) unit (Shimadzu Prominence, Kyoto, Japan), an SEC column [Shodex column (SB-803 HQ)], and a mobile phase of 75% phosphate buffer +25% acetonitrile (Wako Pure Chemicals Ltd., Osaka, Japan) adjusted to $\text{pH } 7$. Detection of NOM was achieved with a UV detector set at 254 nm. Poly(styrene sulfonate) (PSS) standards (1.0, 4.6, 18, and 67 kDa) were purchased from Polyscience Inc. and were used as standard molecular weights. Molecular weights and polydispersities were determined according to the method of Chin et al.²¹ It should be noted that the calculated average molecular weight values obtained by HPSEC with UV–vis detectors are skewed by the SUVA of the DOC. Variations in molecular-weight values obtained by HPSEC in different studies are due to changes in the mobile phases, electrostatic repulsion, and column type; nevertheless, SEC is a useful technique for comparing changes in molecular weights among different samples.²²

Excitation–emission matrix (EEM) fluorescence was measured as described by Murphy et al.²³ using an RF-5300 fluorescence spectrometer (Shimadzu Corp., Kyoto, Japan) and a quartz cuvette (1-cm path length). Raw EEM data were collected from 240 to 450 nm for excitation (Ex, at 5-nm intervals) and from 300 to 600 nm for emission (Em, at 2-nm intervals). EEM spectra were processed by spectral correction, inner-filter correction, Raman correction, and quinine sulfate calibration and then analyzed using the FDOMcorr toolbox.²³ The excitation–emission pairs (peak picking)²⁴ used in this study are described in Table S2. Fluorescence intensities are reported in Raman units (RU). The fluorescence index (FI)

was calculated as the ratio of the emission intensity at Em 450 nm relative to that at Em 500 nm at Ex 370 nm. The freshness index (BIX) was calculated by taking the intensity ratio of Em 380 nm relative to that of Em 430 nm at Ex 310 nm.²⁵

3. RESULTS AND DISCUSSION

3.1. Characterization of NOM. Variations in the molecular composition (i.e., percentages of C, O, and H) of the NOM

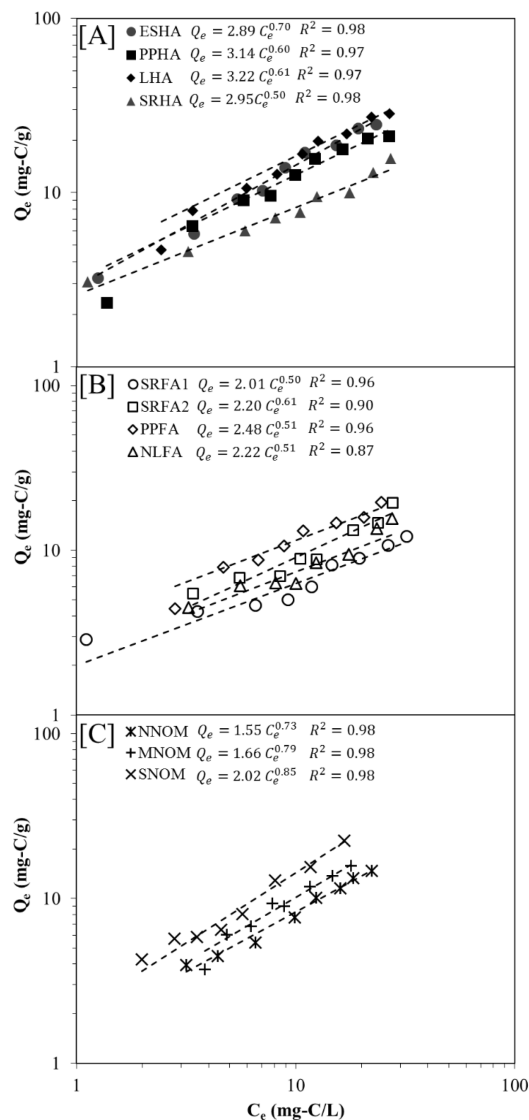


Figure 1. Isotherm results for (A) humic acids, (B) fulvic acids, and (C) RO isolates used in this study. The initial NOM concentration was increased at fixed CNT dose ($C1/SSA = 134\text{ m}^2/\text{g}$) at 250 (mg of CNT)/L and at the same equilibrium time of 24 h. Experimental data were fitted to the Freundlich model (dashed line).

used in this study are reported in Table S1. Generally, the carbon content was higher in the humic acids than in the fulvic acids and RO isolates, and the oxygen content was high for the NOM from aquatic sources. The heterogeneity of natural organic matter depends on its source (e.g., aquatic, soil-based), which also influences its adsorption behavior.²⁶ The sources of the NOM used in this study included soil (one humic acid), leonardite (one humic acid), peat (one humic acid and one

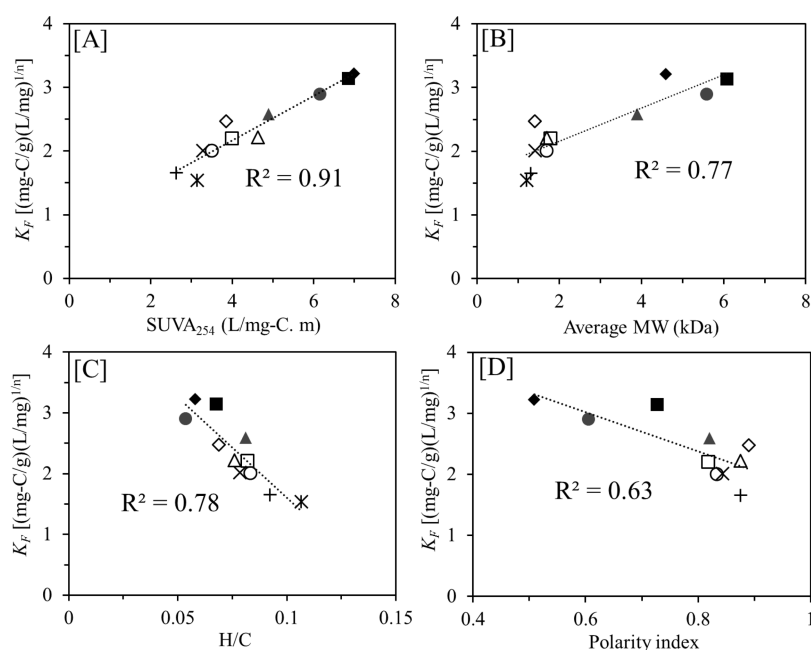


Figure 2. Relationships of the Freundlich constant K_F with (A) $SUVA_{254}$, (B) average molecular weight, (C) H/C atomic ratio, and (D) polarity index [i.e., (O + N)/C atomic ratio] for all NOM used in this study. (Gray solid circles, ESHA; solid squares, PPHA; solid diamonds, LHA; gray solid triangles, SRHA; open circles, SRFA1; open squares, SRFA2; open diamonds, PPFA; open triangles, NLFA; stars, NNOM; +, MNOM; ×, SNOM.)

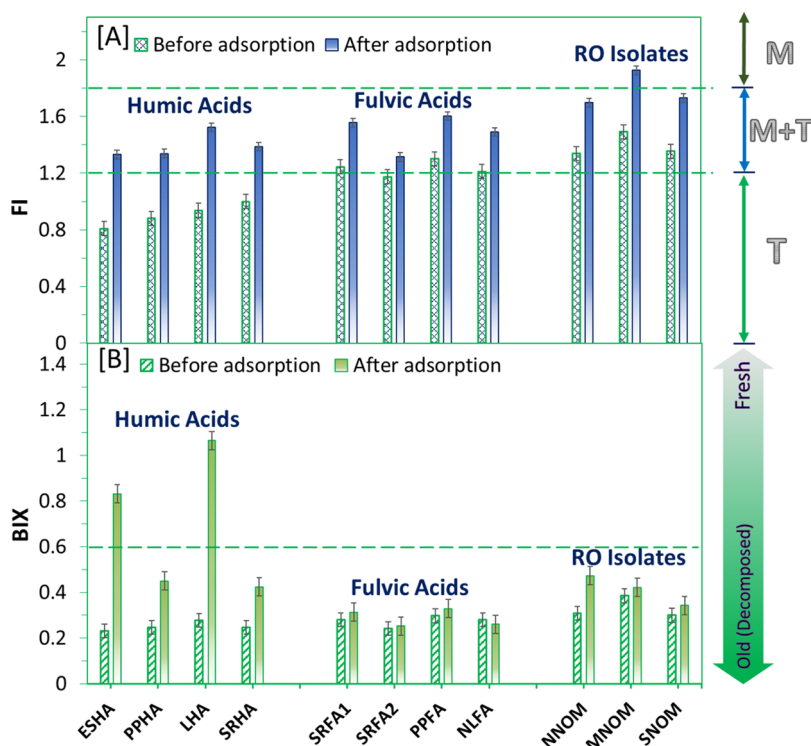


Figure 3. Changes in (A) fluorescence index (FI) and (B) freshness index (BIX) for all NOM samples in this study. C_e was 2–3 (mg of C)/L, the equilibrium time was 24 h, and the sample pH was 7 ± 0.2 . T, terrestrial-derived DOM; M, microbial-derived DOM.

185 fulvic acid), and aquatic sources from rivers and lakes (one
186 humic acid, three fulvic acids, and three RO isolates).

187 Other major differences among the NOM samples were the
188 $SUVA_{254}$ values and the average molecular weights (Figures S1
189 and S2). Aromaticity, as indicated by $SUVA_{254}$, was higher for
190 the humic acids [4.9–7.0 L/(mg m)] (LHA > PPHA > ESHA
191 > SRHA) than for the fulvic acids [3.4–4.6 L/(mg m)] (NLFA

> SRFA2 > PPFA > SRFA1) and RO isolates [2.6–3.6 L/(mg
192 m)] (SRNOM > NNOM > MNOM) (Table 1). This trend is
193 in agreement with those reported in previous studies by Hyung
194 and Kim¹⁰ and Rodríguez and Núñez.²⁷ To the best of our
195 knowledge, among the total of 11 NOM samples used in this
196 study, the average molecular weights of only five (i.e., ESHA,
197 LHA, SRHA, SRFA1, and SRFA2) were previously reported, 198

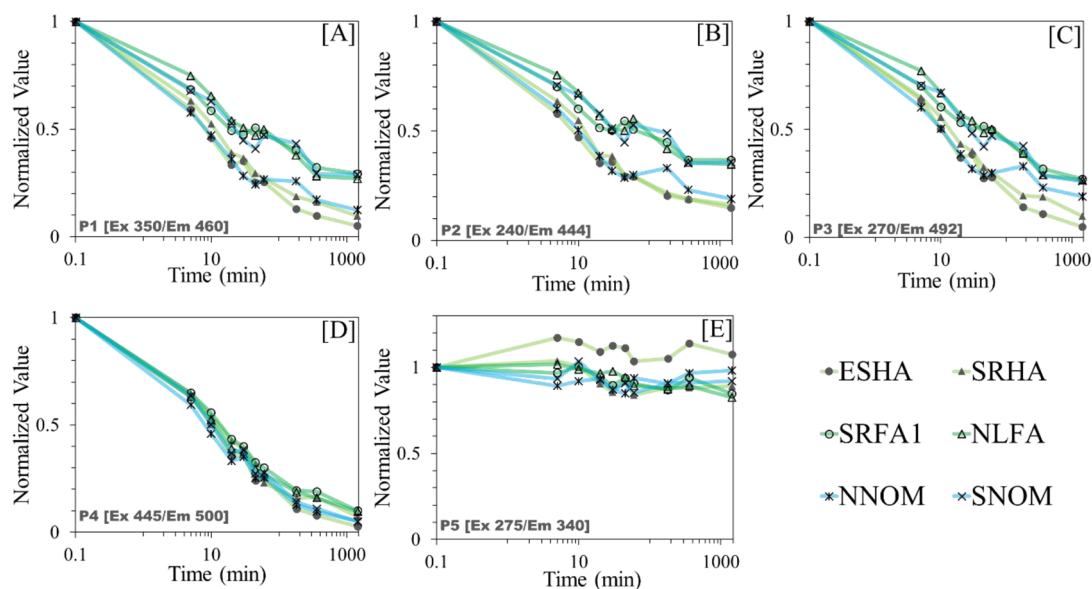


Figure 4. Kinetics of EEM peaks (P1–P5) for NNOM, SNOM, SRFA1, NLFA, ESHA, and SRHA. The initial NOM concentration was 5 mg/L, the CNT concentration was 250 mg/L, and the sample pH was 7 ± 0.2 .

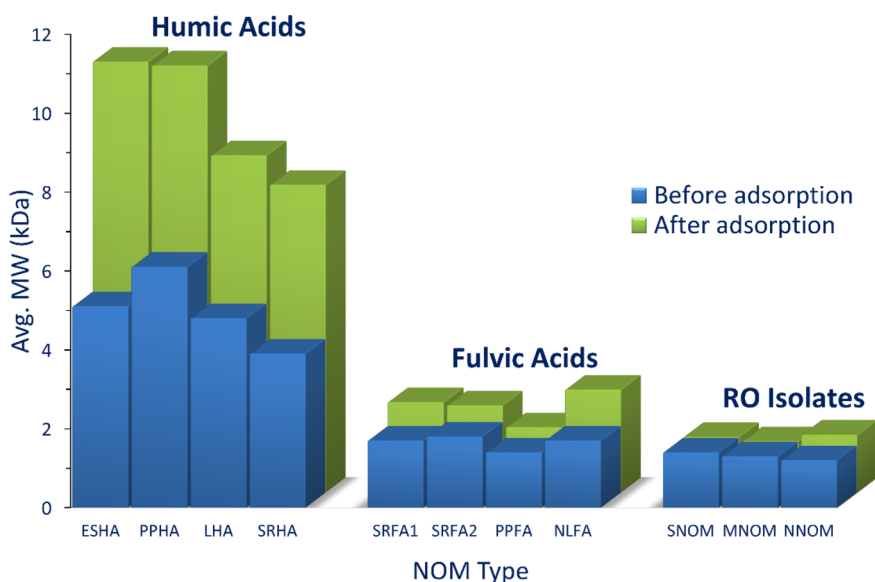


Figure 5. Changes in the average molecular weight for the samples of natural organic matter used in this study. C_e was 2–3 (mg of C)/L, the equilibrium time was 24 h, and the sample pH was 7 ± 0.2 .

199 and the previously reported values showed, in general, good
 200 agreement with our measurements.^{2,28–31} We also note that
 201 some previous studies reported incomparable average molec-
 202 ular weight values for some of the IHSS standard NOM
 203 samples; thus, these values were excluded from the comparison.
 204 For example, we found that average molecular weights reported
 205 for NLFA by Persson et al.,³² for ESHA by Heo et al.,³³ and for
 206 SNOM by Wagoner et al.³⁴ were approximately 300%, 400%,
 207 and 1200% higher, respectively, than our average values.
 208 However, specific reasons for the overestimation of the values
 209 in those studies were not obvious because (1) some studies did
 210 not report some details of sample preparation (indicated by
 211 “N.A.” in Table S3) and (2) the number of samples in each
 212 study was limited. A detailed comparison of the results and
 213 experimental conditions between this and previous studies is
 214 summarized in Table S3.

The EEM method is frequently being used for NOM 215
 characterization in water because of its high sensitivity, good 216
 selectivity, and preservation of samples.³⁵ Therefore, two EEM 217
 indexes, FI and BIX, were used to categorize the source and age 218
 of the NOM samples in this work. FI tracks the source of NOM 219
 as microbial-derived (e.g., organic matter from aquatic 220
 microorganisms) or terrestrially derived.³⁶ NOM samples 221
 with FI values greater than 1.8 and less than 1.2 are classified 222
 as microbial-derived NOM and terrestrial-derived NOM, 223
 respectively.²⁵ FI values between 1.2 and 1.8 indicate that the 224
 NOM is a mixture of microbial and terrestrial aquatic 225
 substances. In the present study, the FI values were higher 226
 for the fulvic acids (FAs) (1.16–1.29) and RO isolates (1.33– 227
 1.49) than for the humic acids (HAs) (0.84–1.0) (Table 1). 228
 Higher FI values for FAs than for HAs were previously reported 229
 by Rodríguez et al.,³⁷ and to the best of our knowledge, FI 230

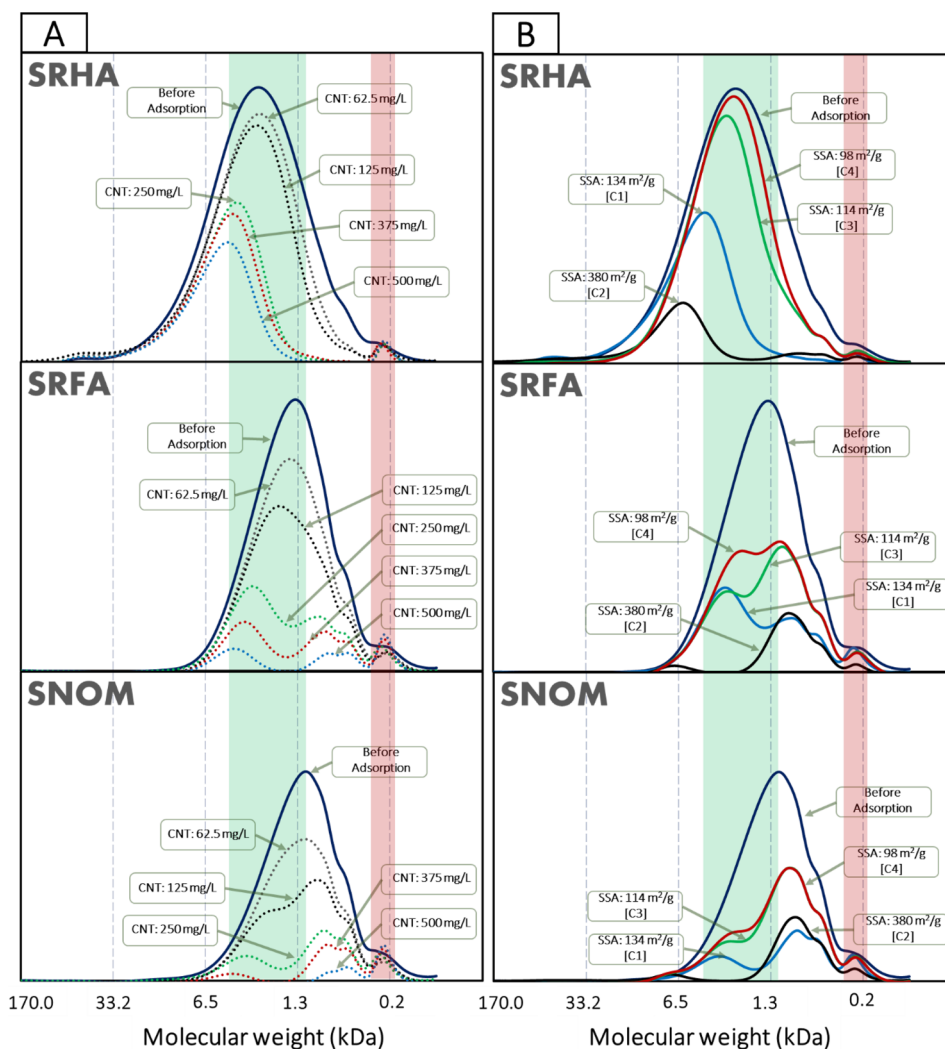


Figure 6. Molecular weight distributions for adsorption experiments with Suwanee River humic acid, fulvic acid, and RO isolates for (A) experiments at the same initial NOM concentration (10 mg/L) with five different CNT doses of one type of CNT (C1, 134 m²/g) and (B) experiments with four different types of CNTs (C2, SWCNTs; C1, C3, and C4, MWCNTs) at the same initial NOM concentration (10 mg/L) with the same CNT dose [250 (mg of CNT)/L]. Green color highlights the molecular weight range for the preferentially adsorbed fraction. Red color highlights the molecular weight range for the non-preferred fraction.

231 values for standard IHSS RO isolates have not previously been
 232 reported in the literature. BIX is called the index of recent
 233 autochthonous contribution and can be determined as the ratio
 234 between the recently derived NOM and the decomposed (i.e.,
 235 older) NOM.³⁸ According to the BIX classification, all of the
 236 NOM samples used in the present study appeared to be
 237 decomposed, with BIX values of less than 0.6, and none was
 238 freshly produced (BIX > 1) (Table 1). The BIX values for IHSS
 239 samples were reported to fall in the same range, between 0.2
 240 and 0.4, in previous studies.³⁹ The NOM samples were further
 241 characterized based on EEM peaks (Table S2) and showed
 242 variations in component compositions (P1–P5), as illustrated
 243 in Figure S3. Detailed characterizations of the EEM peaks in
 244 this study are provided in section S2 of the SI.

245 **3.2. Effect of NOM Molecular Properties on the**
 246 **Adsorption Affinity.** The results of adsorption isotherm
 247 measurements and application of the Freundlich model for 11
 248 NOM samples on four CNTs are presented in Table S4. The
 249 Freundlich model is described by the equation

$$250 \quad Q_e = K_F C_e^{1/n} \quad (1)$$

where Q_e [(mg of C)/g] is the adsorption affinity, C_e [(mg of 251
 C)/L] is the equilibrium concentration, K_F {[(mg of C)/g]/ 252
 [(mg of C)/L]^{1/n}} is the Freundlich constant, and 1/n is the 253
 Freundlich exponent. 254

Figure 1 shows the results of adsorption isotherm experi- 255
 ments for MWCNT C1 (Table 2). The Freundlich model 256
 showed a good fit with the isotherm data, as indicated by the 257
 coefficients of determination (R^2) ranging between 0.87 and 258
 0.98 (Table S4), which agrees with previous reports of NOM 259
 adsorption on activated carbon,² carbon nanotubes,¹⁰ and 260
 graphene nanomaterials.³ 261

Based on the NOM sources, the adsorption capacities 262
 followed the order leonardite > peat > soil > aquatic. According 263
 to NOM type, the adsorption affinity of the humic acids was 264
 generally higher than that of the fulvic acids (Figure 1 and 265
 Table S4). This difference can be attributed to the higher 266
 aromaticity of the humic acids, as indicated by their SUVA₂₅₄ 267
 values (Table 1). Similar trends were previously reported for 268
 the adsorption of NOM by graphene and MWCNTs.^{3,10} 269
 Among the NOM characteristics, SUVA₂₅₄, an indicator of 270
 aromaticity, showed a strong linear relationship with K_F 271

regardless of the source and type of NOM (Figures 2A and S4).¹⁰ The adsorption affinity was found to be inversely proportional to the H/C atomic ratio and the polarity index [i.e., the (O + N)/C atomic ratio] (see Figures 2C,D and S5). These findings show that hydrophobic repulsion from water and π - π attractions are the main driving forces for adsorption between NOM and CNTs. In addition, the carboxylic acidity of the NOM showed a negative correlation with the adsorption affinity (Figure S6). A similar trend was previously reported for the adsorption of NOM samples with different carboxylic acidities on granular activated carbon.² Finally, NOM samples with higher average molecular weights exhibited higher adsorption affinities (Figure 2B); however, a detailed analysis of the effect of molecular weight will not be discussed further until section 3.4.

All adsorption results were also processed for the adsorption affinity (Q_e) at three different equilibrium concentrations [$C_e = 5 \pm 1$, 11 ± 1 , and 22 ± 1 (mg of C)/L]. According to our analysis, the examined adsorption capacities showed trends similar to those of K_F for the tested parameters. (See Figures S4–S6.)

Because of the oxygen-containing groups on their surface, CNTs have more hydrophilic character, which can result in the reduction of their adsorption capacities for organic compounds.⁴⁰ However, the surface oxygen contents of the CNTs used in this study fell in a narrow range (i.e., 0.21–0.30 wt % for the MWCNTs and 1.3 wt % for the SWCNTs) (Table 2). Thus, the dependence of the adsorption on the physical characteristics of the CNTs (i.e., surface area and pore size) was examined and is discussed in section S3 of the SI. The BET results showed that the CNTs had different surface areas (98–380 m²/g) and pore volumes (0.4–0.9 cm³/g) (Table 2). Because micropores (<2 nm) are not likely to be accessible to all NOM molecules,¹² only mesopores (2 nm > PV > 50 nm) and macropores (PV > 50 nm) were taken into account. Basically, the sorption coefficient ($K_d = Q/C_e$) was normalized to the surface areas and pore volumes of four different CNT samples (i.e., one SWCNT sample and three MWCNT samples) to adsorb SRHA, SRFA1, and SNOM. Wang et al.¹² reported that, in addition to the effect of pore size, that normalized adsorption affinity increased when they used CNTs with large outer diameters (ODs). This can be linked to the enhanced dispersion of CNTs with large ODs compared to those with small ODs⁴¹ and/or the lower curvature of the surface of large-OD CNTs, allowing for better alignment of the adsorbate molecules.⁴²

3.3. Preferential Adsorption Related to the Source and Age of NOM. Lavonen et al.⁴³ reported FI to be a good indicator for investigating the changes in NOM occurring during several different treatment processes in water treatment plants (e.g., coagulation, filtration, disinfection). Similarly, Rodríguez et al.³⁷ employed FI to monitor the compositional changes in humic substances after ozonation treatments. In another study, Kothawala et al.⁴⁴ used FI to evaluate the characteristics of NOM after sorption onto soil particles. In the present study, as reported in Table 1, the FI values for the bulk samples of NOM (i.e., before adsorption) indicated that all of the HAs were more likely to be terrestrial-derived NOM (FI < 1.2). However, the FAs and RO isolates shared the characteristics of mixtures of both terrestrial and microbial aquatic NOM (1.2 < FI < 1.8).^{25,45} Figure 3A shows that the FI values for all NOM types increased after adsorption (FI > 1.2). This is an indication of the preferential adsorption of terrestrial-derived

compounds. Such a finding is consistent with the notion that NOM samples with low FI values are rich in aromatic moieties (Figure S7A), as previously reported by Ateia et al.⁴⁶ and Shimabuku et al.²⁰ A high negative correlation ($R^2 = 0.89$) was also found between the FI values and the average molecular weights of all NOM samples (Figure S7B). This confirms the adsorption results reported in the previous section, where the adsorption affinity of the NOM types with high average molecular weights (i.e., HAs) was higher than that of the NOM types with lower average molecular weights (i.e., FAs and RO isolates).

In contrast to the results for FI, an increasing trend in BIX was observed only for HAs, whereas the BIX values changed only slightly for FAs and RO isolates after adsorption onto the CNTs. The BIX increments were more pronounced for ESHA and LHA, followed by PPHA and SRHA (Figure 3B); however, the overall trend illustrates the preferential adsorption for decomposed NOM fractions over freshly produced NOM. According to Hunt and Ohno⁴⁷ and Wang et al.,⁴⁸ one possible reason for this is that decomposed fractions (i.e., those with low BIX values) have higher C/N ratios and higher aromaticity than freshly produced NOM. Further, Figure S8 illustrates the gradual changes in FI and BIX with time in kinetic adsorption experiments using six NOM samples (i.e., ESHA, SRHA, SRFA, NLFA, NNOM, and SNOM). From these results, one can see that FI is more sensitive and would be more suitable for describing and tracking the changes in NOM composition.

NOM is a heterogeneous mixture of complex organic compounds. Therefore, preferentially adsorbed portions of NOM dominate the adsorption behavior at low concentrations, and the adsorption process would be limited by the available adsorption sites (i.e., surface area) at elevated NOM concentrations.¹⁰ In this regard, further analysis showed that the variations in FI and BIX were also concentration-dependent. As shown in Figures S9 and S10, the changes in FI and BIX were pronounced at equilibrium concentrations (C_e) of up to 5 (mg of C)/L; however, at high concentrations, the FI and BIX values were similar to the original values before adsorption. Thus, the fluorescence index can serve as an easy and practical metric for tracking NOM fractionation during the adsorption process on CNTs.

Although EEM fluorescence has been applied successfully to track the changes in NOM compositions after biological⁴³ and physical³⁷ treatment processes, very few studies have utilized this technique as a tracking tool for NOM preferential adsorption on graphene nanomaterials (e.g., see the articles by Peng et al.¹⁷ and Lee et al.²⁶). In the current study, five EEM peaks with different pairs reflected several fractions with variations in NOM source and size (Figure S3 and Table S2).^{36,49} Figure 4 shows the normalized removal of each fraction for six NOM samples as a function of time. The terrestrial and hydrophobic components showed the highest preferential adsorption. The same observation was reported for the adsorption of landfill leachate on activated carbon⁵⁰ and soil-derived HAs on graphene oxide.²⁶ It also supports the conclusion based on the FI values that terrestrial fractions are preferentially adsorbed compared to microbial NOM. Interestingly, the intensity of P5 (Ex 270/Em 492) (Figure 4E) did not decrease after the adsorption of all of the NOM tested in this study on CNTs. This peak represents aromatic amino acids (protein-like or tryptophan-like components).^{25,26} This observation was further examined by checking the molecular

397 weights of the residual fractions, as discussed in detail in the
398 next section.

399 **3.4. Preferential Adsorption Based on the Average**
400 **Molecular Weight of NOM.** NOM contains mixtures of
401 compounds that vary in aromatic content and adsorption
402 capacity. Among the NOM types used in this study, all humic
403 acids, with a wider molecular weight range (0.2–90 kDa) and
404 higher polydispersities ($\rho = 2.7\text{--}5.8$), showed similar
405 preferential adsorption in the molecular weight range between
406 0.5 and 2 kDa. Meanwhile, the adsorption in the range of
407 molecular weights greater than 1 kDa was more preferable for
408 all fulvic acids and RO isolates, which had a narrower molecular
409 weight (0.2–10 kDa) and lower polydispersities ($\rho = 1.5\text{--}1.9$)
410 (Figure S11). Thus, the molecular weight distribution was
411 changed after adsorption, which was clearly reflected in the
412 average molecular weights of the residual fractions (Figure 5).
413 According to Gotovac et al.,⁵¹ a higher number of benzene
414 rings in the aromatic structure of a specific fraction increases its
415 adsorption affinity on CNTs. This selectivity was examined and
416 tracked as a function of time, as visualized in Figure S12.
417 Further, the selective behavior was confirmed in two ways: (1)
418 by increasing the CNT dose (increasing the SSA) (Figure 6A)
419 and (2) by performing adsorption on different types of CNTs
420 (Figure 6B). Previous studies on NOM adsorptive fractions on
421 CNTs or graphene oxides reported only that the high-
422 molecular-weight fractions are more preferable for adsorption.
423 However, those studies drew their conclusions based solely on
424 aquatic NOM^{3,10} or soil FAs,¹¹ and details about the changes in
425 NOM molecular composition (e.g., average molecular weight,
426 molecular weight distribution, and polydispersity) were not
427 reported.

428 Another observation in this study was the “selective”
429 adsorption on CNTs of the fraction with molecular weights
430 of 1–3 kDa from the bulk samples of FAs and RO isolates
431 (Figures 6, S11, and S12). According to Lv et al.,⁵² this fraction
432 is likely to comprise aromatic molecular groups, based on a
433 comparison of the results of HPSEC and Fourier transform ion
434 cyclotron resonance mass spectrometry (FT-ICR-MS). In
435 another study, Li et al.¹⁹ tested the adsorption by CNTs of
436 styrene sulfonate (SS) and poly(styrene sulfonate) (PSS)
437 samples with different molecular weight values (0.2, 4.3, 6.8,
438 10.0, 17.0, and 70.0 kDa) and found the highest adsorption
439 capacity for PSSs with an average molecular weight of 4.7 kDa.
440 It is important to highlight that, based on HPSEC, the small
441 fraction (MW < 0.4 kDa) did not adsorb on the CNTs (Figures
442 6, S11, and S12). This finding supports the EEM results and
443 can be linked to protein-like compounds (Figure 4E), which
444 were also not removed by the CNTs. Cai et al.³ reported the
445 same lack of uptake of the small fraction for the adsorption of
446 NOM on graphene oxides. Therefore, we conclude that NOM
447 fractions with molecular weights of <0.4 kDa are more likely to
448 be hydrophilic compounds that cannot adsorb on CNTs.²²

449 In this study, the comprehensive characterization of NOM
450 before and after adsorption along with the characterization of
451 CNTs provided important insights into the adsorption of
452 NOM on CNTs. The results indicate that FI can serve as an
453 easy and practical metric for describing and tracking the
454 fractionation of NOM during the adsorption process. Selective
455 adsorption in the molecular weight range of 0.5–2 kDa for
456 humic acids and in the molecular weight range of 1–3 kDa for
457 all fulvic acids and RO isolates was also revealed. Given the
458 wide variety of NOM samples in aquatic and soil environments,
459 the findings of this study further help to clarify and predict the

adsorption behavior of NOM samples on CNTs in natural
waters and/or the potential application of CNTs for water
treatment. However, further studies to examine and identify the
adsorption fractions of NOM by CNTs using sensitive
techniques (e.g., mass spectroscopy) are still needed to
elucidate the factors controlling the adsorption behavior of
this complex type of material.

■ ASSOCIATED CONTENT

📄 Supporting Information

The Supporting Information is available free of charge on the
ACS Publications website at DOI: 10.1021/acs.est.7b01279.

Adsorption kinetics (section S1, Table S5, Figure S13).
EEM peaks description (section S2, Table S2, Figure S3).
Effects of CNT surface area and pore volume on
adsorption (section S3, Figures S14 and S15). NOM
characteristics (Table S1). HPSEC results (Table S3,
Figures S1, S11, and S12). Freundlich isotherm results
(Table S4). SUVA₂₅₄ vs average molecular weight
(Figure S2). K_F vs NOM molecular properties (Figures
S4–S6). FI vs SUVA₂₅₄ and average molecular weight
(Figure S7). FI and BIX values at different times (Figure
S8) and with increasing concentrations (Figures S9 and
S10) (PDF)

■ AUTHOR INFORMATION

Corresponding Author

*Phone: 0081-80-3430-9753; e-mail: mohamedateial@gmail.com.

ORCID

Mohamed Ateia: 0000-0002-3524-5513

Notes

The authors declare no competing financial interest.

■ ACKNOWLEDGMENTS

This work was supported in part by the Program for Leading
Graduate School “Academy for Co-creative Education of
Environment and Energy Science”, MEXT, Tokyo Institute of
Technology, and JSPS Core-to-Core Program. We thank
Mahmut Ersan, Department of Environmental Engineering
and Earth Science, Clemson University, for providing BET
results.

■ REFERENCES

- (1) Engel, M.; Chefetz, B. Adsorption and desorption of dissolved organic matter by carbon nanotubes: Effects of solution chemistry. *Environ. Pollut.* **2016**, *213*, 90–98.
- (2) Karanfil, T.; Kilduff, J. E.; Schlautman, M. A.; Weber, W. J. Adsorption of organic macromolecules by granular activated carbon. 1. Influence of molecular properties under anoxic solution conditions. *Environ. Sci. Technol.* **1996**, *30* (7), 2187–2194.
- (3) Cai, N.; Peak, D.; Larese-Casanova, P. Factors influencing natural organic matter sorption onto commercial graphene oxides. *Chem. Eng. J.* **2015**, *273*, 568–579.
- (4) Karanfil, T.; Kilduff, J. E.; Schlautman, M. A.; Weber, W. J., Jr. The oxygen sensitivity of organic macromolecule sorption by activated carbon: effects of solution chemistry. *Water Res.* **1998**, *32* (1), 154–164.
- (5) Bhatnagar, A.; Sillanpää, M. Removal of natural organic matter (NOM) and its constituents from water by adsorption—A review. *Chemosphere* **2017**, *166*, 497–510.

- (6) Santhosh, C.; Velmurugan, V.; Jacob, G.; Jeong, S. K.; Grace, A. N.; Bhatnagar, A. Role of nanomaterials in water treatment applications: A review. *Chem. Eng. J.* **2016**, *306*, 1116–1137.
- (7) Ahmadi, M.; Elmongy, H.; Madrakian, T.; Abdel-Rehim, M. Nanomaterials as sorbents for sample preparation in bioanalysis: A review. *Anal. Chim. Acta* **2017**, *958*, 1–21.
- (8) Apul, O. G.; Karanfil, T. Adsorption of synthetic organic contaminants by carbon nanotubes: A critical review. *Water Res.* **2015**, *68*, 34–55.
- (9) Smith, S. C.; Rodrigues, D. F. Carbon-based nanomaterials for removal of chemical and biological contaminants from water: a review of mechanisms and applications. *Carbon* **2015**, *91*, 122–143.
- (10) Hyung, H.; Kim, J.-H. Natural organic matter (NOM) adsorption to multi-walled carbon nanotubes: effect of NOM characteristics and water quality parameters. *Environ. Sci. Technol.* **2008**, *42* (12), 4416–4421.
- (11) Yang, K.; Xing, B. Adsorption of fulvic acid by carbon nanotubes from water. *Environ. Pollut.* **2009**, *157* (4), 1095–1100.
- (12) Wang, X.; Shu, L.; Wang, Y.; Xu, B.; Bai, Y.; Tao, S.; Xing, B. Sorption of peat humic acids to multi-walled carbon nanotubes. *Environ. Sci. Technol.* **2011**, *45* (21), 9276–9283.
- (13) Lin, D.; Li, T.; Yang, K.; Wu, F. The relationship between humic acid (HA) adsorption on and stabilizing multiwalled carbon nanotubes (MWNTs) in water: effects of HA, MWNT and solution properties. *J. Hazard. Mater.* **2012**, *241-242*, 404–410.
- (14) Wang, F.; Yao, J.; Chen, H.; Yi, Z.; Xing, B. Sorption of humic acid to functionalized multi-walled carbon nanotubes. *Environ. Pollut.* **2013**, *180*, 1–6.
- (15) Engel, M.; Chefetz, B. Adsorptive fractionation of dissolved organic matter (DOM) by carbon nanotubes. *Environ. Pollut.* **2015**, *197*, 287–294.
- (16) Zhang, D.; Pan, B.; Cook, R. L.; Xing, B. Multi-walled carbon nanotube dispersion by the adsorbed humic acids with different chemical structures. *Environ. Pollut.* **2015**, *196*, 292–299.
- (17) Peng, M.; Li, H.; Li, D.; Du, E.; Li, Z. Characterization of DOM adsorption of CNTs by using excitation–emission matrix fluorescence spectroscopy and multiway analysis. *Environ. Technol.* **2017**, *38*, 1351–1361.
- (18) Chen, W.; Duan, L.; Zhu, D. Adsorption of polar and nonpolar organic chemicals to carbon nanotubes. *Environ. Sci. Technol.* **2007**, *41* (24), 8295–8300.
- (19) Li, T.; Lin, D.; Li, L.; Wang, Z.; Wu, F. The kinetic and thermodynamic sorption and stabilization of multiwalled carbon nanotubes in natural organic matter surrogate solutions: the effect of surrogate molecular weight. *Environ. Pollut.* **2014**, *186*, 43–49.
- (20) Shimabuku, K. K.; Kennedy, A. M.; Mulhern, R. E.; Summers, R. S. Evaluating Activated Carbon Adsorption of Dissolved Organic Matter and Micropollutants Using Fluorescence Spectroscopy. *Environ. Sci. Technol.* **2017**, *51* (5), 2676–2684.
- (21) Chin, Y.-P.; Aiken, G.; O’Loughlin, E. Molecular weight, polydispersity, and spectroscopic properties of aquatic humic substances. *Environ. Sci. Technol.* **1994**, *28* (11), 1853–1858.
- (22) Sandron, S.; Rojas, A.; Wilson, R.; Davies, N. W.; Haddad, P. R.; Shellie, R. A.; Nesterenko, P. N.; Kelleher, B. P.; Paull, B. Chromatographic methods for the isolation, separation and characterisation of dissolved organic matter. *Environmental Science: Processes & Impacts* **2015**, *17* (9), 1531–1567.
- (23) Murphy, K. R.; Butler, K. D.; Spencer, R. G.; Stedmon, C. A.; Boehme, J. R.; Aiken, G. R. Measurement of dissolved organic matter fluorescence in aquatic environments: an interlaboratory comparison. *Environ. Sci. Technol.* **2010**, *44* (24), 9405–9412.
- (24) Coble, P. G. Characterization of marine and terrestrial DOM in seawater using excitation-emission matrix spectroscopy. *Mar. Chem.* **1996**, *51* (4), 325–346.
- (25) Coble, P. G.; Lead, J.; Baker, A.; Reynolds, D. M.; Spencer, R. G. M., Eds. *Aquatic Organic Matter Fluorescence*; Cambridge Environmental Chemistry Series; Cambridge University Press: New York, 2014.
- (26) Lee, B.-M.; Seo, Y.-S.; Hur, J. Investigation of adsorptive fractionation of humic acid on graphene oxide using fluorescence EEM-PARAFAC. *Water Res.* **2015**, *73*, 242–251.
- (27) Rodríguez, F. J.; Núñez, L. A. Characterization of aquatic humic substances. *Water Environ. J.* **2011**, *25* (2), 163–170.
- (28) Zhou, Q.; Cabaniss, S. E.; Maurice, P. A. Considerations in the use of high-pressure size exclusion chromatography (HPSEC) for determining molecular weights of aquatic humic substances. *Water Res.* **2000**, *34* (14), 3505–3514.
- (29) Chin, Y.-P.; Aiken, G. R.; Danielsen, K. M. Binding of pyrene to aquatic and commercial humic substances: the role of molecular weight and aromaticity. *Environ. Sci. Technol.* **1997**, *31* (6), 1630–1635.
- (30) Hur, J.; Schlautman, M. A. Using selected operational descriptors to examine the heterogeneity within a bulk humic substance. *Environ. Sci. Technol.* **2003**, *37* (5), 880–887.
- (31) McKay, G.; Kleinman, J. L.; Johnston, K. M.; Dong, M. M.; Rosario-Ortiz, F. L.; Mezyk, S. P. Kinetics of the reaction between the hydroxyl radical and organic matter standards from the International Humic Substance Society. *J. Soils Sediments* **2014**, *14* (2), 298–304.
- (32) Persson, L.; Alsberg, T.; Ledin, A.; Odham, G. Transformations of dissolved organic matter in a landfill leachate—a size exclusion chromatography/mass spectrometric approach. *Chemosphere* **2006**, *64* (7), 1093–1099.
- (33) Heo, J.; Yoon, Y.; Kim, D.-H.; Lee, H.; Lee, D.; Her, N. A new fluorescence index with a fluorescence excitation-emission matrix for dissolved organic matter (DOM) characterization. *Desalin. Water Treat.* **2016**, *57* (43), 20270–20282.
- (34) Wagoner, D. B.; Christman, R. F.; Cauchon, G.; Paulson, R. Molar mass and size of Suwannee River natural organic matter using multi-angle laser light scattering. *Environ. Sci. Technol.* **1997**, *31* (3), 937–941.
- (35) Li, W.-T.; Chen, S.-Y.; Xu, Z.-X.; Li, Y.; Shuang, C.-D.; Li, A.-M. Characterization of dissolved organic matter in municipal wastewater using fluorescence PARAFAC analysis and chromatography multi-excitation/emission scan: a comparative study. *Environ. Sci. Technol.* **2014**, *48* (5), 2603–2609.
- (36) McKnight, D. M.; Boyer, E. W.; Westerhoff, P. K.; Doran, P. T.; Kulbe, T.; Andersen, D. T. Spectrofluorometric characterization of dissolved organic matter for indication of precursor organic material and aromaticity. *Limnol. Oceanogr.* **2001**, *46* (1), 38–48.
- (37) Rodríguez, F. J.; Schlenger, P.; García-Valverde, M. A comprehensive structural evaluation of humic substances using several fluorescence techniques before and after ozonation. Part I: Structural characterization of humic substances. *Sci. Total Environ.* **2014**, *476-477*, 718–730.
- (38) Huguet, A.; Vacher, L.; Relexans, S.; Saubusse, S.; Froidefond, J.-M.; Parlanti, E. Properties of fluorescent dissolved organic matter in the Gironde Estuary. *Org. Geochem.* **2009**, *40* (6), 706–719.
- (39) Birdwell, J. E.; Engel, A. S. Characterization of dissolved organic matter in cave and spring waters using UV–Vis absorbance and fluorescence spectroscopy. *Org. Geochem.* **2010**, *41* (3), 270–280.
- (40) Apul, O. G.; Wang, Q.; Zhou, Y.; Karanfil, T. Adsorption of aromatic organic contaminants by graphene nanosheets: Comparison with carbon nanotubes and activated carbon. *Water Res.* **2013**, *47* (4), 1648–1654.
- (41) Lin, D.; Xing, B. Tannic acid adsorption and its role for stabilizing carbon nanotube suspensions. *Environ. Sci. Technol.* **2008**, *42* (16), 5917–5923.
- (42) Apul, O. G.; Shao, T.; Zhang, S.; Karanfil, T. Impact of carbon nanotube morphology on phenanthrene adsorption. *Environ. Toxicol. Chem.* **2012**, *31* (1), 73–78.
- (43) Lavonen, E.; Kothawala, D.; Tranvik, L.; Gonsior, M.; Schmitt-Kopplin, P.; Köhler, S. Tracking changes in the optical properties and molecular composition of dissolved organic matter during drinking water production. *Water Res.* **2015**, *85*, 286–294.
- (44) Kothawala, D.; Roehm, C.; Blodau, C.; Moore, T. Selective adsorption of dissolved organic matter to mineral soils. *Geoderma* **2012**, *189-190*, 334–342.

- 654 (45) Cory, R. M.; McKnight, D. M.; Chin, Y.-P.; Miller, P.; Jaros, C.
655 L. Chemical characteristics of fulvic acids from Arctic surface waters:
656 Microbial contributions and photochemical transformations. *Journal of*
657 *Geophysical Research: Biogeosciences* **2007**, *112*, G04S51.
- 658 (46) Ateia, M.; Ran, J.; Fujii, M.; Yoshimura, C. The relationship
659 between molecular composition and fluorescence properties of humic
660 substances. *Int. J. Environ. Sci. Technol.* **2017**, *14*, 867–880.
- 661 (47) Hunt, J. F.; Ohno, T. Characterization of fresh and decomposed
662 dissolved organic matter using excitation-emission matrix fluorescence
663 spectroscopy and multiway analysis. *J. Agric. Food Chem.* **2007**, *55* (6),
664 2121–2128.
- 665 (48) Wang, Y.-L.; Yang, C.-M.; Zou, L.-M.; Cui, H.-Z. Spatial
666 distribution and fluorescence properties of soil dissolved organic
667 carbon across a riparian buffer wetland in Chongming Island, China.
668 *Pedosphere* **2015**, *25* (2), 220–229.
- 669 (49) Hertkorn, N.; Benner, R.; Frommberger, M.; Schmitt-Kopplin,
670 P.; Witt, M.; Kaiser, K.; Kettrup, A.; Hedges, J. I. Characterization of a
671 major refractory component of marine dissolved organic matter.
672 *Geochim. Cosmochim. Acta* **2006**, *70* (12), 2990–3010.
- 673 (50) Lee, S.; Hur, J. Heterogeneous adsorption behavior of landfill
674 leachate on granular activated carbon revealed by fluorescence
675 excitation emission matrix (EEM)-parallel factor analysis (PARAFAC).
676 *Chemosphere* **2016**, *149*, 41–48.
- 677 (51) Gotovac, S.; Honda, H.; Hattori, Y.; Takahashi, K.; Kanoh, H.;
678 Kaneko, K. Effect of nanoscale curvature of single-walled carbon
679 nanotubes on adsorption of polycyclic aromatic hydrocarbons. *Nano*
680 *Lett.* **2007**, *7* (3), 583–587.
- 681 (52) Lv, J.; Zhang, S.; Wang, S.; Luo, L.; Cao, D.; Christie, P.
682 Molecular-Scale Investigation with ESI-FT-ICR-MS on Fractionation
683 of Dissolved Organic Matter Induced by Adsorption on Iron
684 Oxyhydroxides. *Environ. Sci. Technol.* **2016**, *50* (5), 2328–2336.